ResearchGate

See discussions, stats, and author profiles for this publication at: https://www.researchgate.net/publication/245373643

Robust Design of Inertial Measurement Units Based on Accelerometers

Article *in* Journal of Dynamic Systems Measurement and Control · May 2009

DOI: 10.1115/1.3072157

CITATIONS
12

READS
182

3 authors, including:

Luc Baron
Polytechnique Montréal
176 PUBLICATIONS **1,720** CITATIONS

SEE PROFILE

Some of the authors of this publication are also working on these related projects:

Fuzzy Logic Based Decision Support View project

Mechatronics and Robotics Design Support View project

All content following this page was uploaded by Luc Baron on 07 January 2014.

The user has requested enhancement of the downloaded file.

Robust Design of Inertial Measurement Units Based on Accelerometers

Zhongkai Qin, Luc Baron and Lionel Birglen
{zhongkai.qin, luc.baron, lionel.birglen}@polymtl.ca
Department of Mechanical Engineering, École Polytechnique de Montréal, Canada

Abstract

This paper presents a robust design scheme for an inertial measurement unit (IMU) composed only of accelerometers. From acceleration data measured by a redundant set of accelerometers, the IMU proposed in this paper can estimate the linear acceleration, angular velocity and angular acceleration of the rigid-body to which it is attached. The robustness of our method to the uncertainty of the locations of the sensors and the measurement noise is obtained through redundancy and optimal configuration of the onboard sensors. In addition, the fail-diagnostics and fail-safe issues are also addressed for reliable operation.

1 Introduction

An Inertial Measurement Unit, or IMU, is the main component of the guidance system used in vehicles, aircrafts and satellites. Most of current IMUs are based on accelerometers and gyroscopes to sense respectively the linear acceleration and the angular velocity. These data are thereupon acquired by the controller of the guidance system, calculating the navigation parameters, i.e., the linear and angular velocities of the system, and subsequently, its coordinates. Because of recent advances in micro-machining technology, high performance and low cost accelerometers are now available (Yazdi, Ayazi and Najafi 1998). Therefore, it becomes an affordable alternative to design all-accelerometer IMUs, eliminating the gyroscope(s). Indeed, the latter suffers from a complicated fabrication process yielding high cost.

Replacing gyroscopes with accelerometers in navigation system has been proposed decades ago in (DiNapoli 1965). The rotational part of the spatial acceleration field was estimated in (Schuler, Grammatikos and Fegley 1965), using five accelerometers with carefully selected axes. Theoretically, a minimum of six linear accelerometers are required for a complete definition of the kinematic parameters of a rigid-body. However, six-accelerometer designs were unsuccessful in the past, since it is necessary to solve a system of three nonlinear ordinary differential equations to obtain the angular acceleration components, which is mathematically unstable according to the Routh-Hurwicz criterion (Liu 1976). In order to overcome this issue in practice, a nine-accelerometer scheme was proposed in (Padgaonkar, Krieger and King 1975). With this design, the linear and angular acceleration can be directly computed from the sensor data, and angular velocity is further obtained through the integration of the angular acceleration. A novel six-accelerometer setup, where the six sensors are located on the edges of a regular tetrahedron, was designed to achieve a numerical stability comparable to the previous nine-sensor design (Chen, Lee and DeBra 1994). Using this novel design, the angular acceleration is first estimated from sensor measurements; then, the angular velocity is obtained by integration. Finally, the linear acceleration at the center of the tetrahedron is computed from the measurements and the value of the angular velocity. An IMU based on this design was developed for automotive applications (Mostov, Soloviev and Koo 1997). An algorithmic procedure for the computation of the screw parameters of rigid-body motion was presented in (Angeles 1986). This algorithm

has been extended to an all-accelerometer IMU with a kinematically redundant set of triaxial accelerometers by (Parsa, Angeles and Misra 2004). With IMU designs, it is advantageous to use triaxial accelerometers due to their compactness, especially when designing a redundant system. However, the commercially available accelerometers are manufactured with three single-axis sensors mounted orthogonally in the same unit. Therefore, this type of sensor may introduce non-negligible errors if used in IMU due to the offsets between measurement points. Presently, micro-machining technology can manufacture cheap monolithic devices able to sense spatial accelerations (Li, Li, Wang, Hao, Li, Zhang and Wu 2001). Piezo-resistive triaxial accelerometers (Plaza, Chen, Esteve and Lora-Tamayo 1998) with limited sensitivity have been developed by using semiconductor technology and micro-machining technology. Further advance in capacitive technology is expected in the near future to yield higher sensitivity and lower thermal coefficient (Matsumoto, Nishimura, Matsuura and Ishida 1999).

In this paper, a robust design of IMU is proposed, which allows the estimation of the linear acceleration, angular acceleration and angular velocity vectors from accelerometer measurements. Moreover, through redundancy and optimal placement of sensors in the unit, the designed IMU can be endowed with computational robustness and high reliability.

This paper is organized as follows:

- in Section 2, design considerations are presented.
- In Section 3, the computation algorithm associated with IMUs designed using ideal triaxial accelerometers is formulated. Thereupon, a robust design scheme is proposed. Subsequently, the issue of diagnostics of sensor failure and a strategy to improve system reliability are discussed.
- Finally, simulation results are reported in Section 4 to support the theoretical analyses presented in the paper and demonstrate the advantages of system redundancy.

2 Design Considerations

To design an accelerometer-based IMU, a certain number of accelerometers are located at different points of the unit to measure projection of point accelerations along the axis of the sensor. The IMU designer should consider many factors such as the cost of both the sensors and the machining of the IMU, reliability, easiness of the calibration, etc. For instance, it is not a trivial task to solely decide what type of sensor should be used. Indeed, many technologies and setups of acceleration sensors are commercially available, e.g., one-, two- and three-axis piezo-resistive, capacitive or electro-mechanical accelerometers can be selected. Usually single-axis sensors are less expensive than multi-axis units, but on the other hand, employing multi-axis sensors may lead to a lower cost for assembling the unit and a simpler calibration procedure.

The design proposed in this paper aims at obtaining computational robustness and high reliability of the measurements. Therefore, a redundant number of sensors is used. In this case, triaxial accelerometers are preferred because of their compactness and simple calibration. However, there is an issue concerning the actual structure of triaxial accelerometers. Since most current triaxial accelerometers are based on three single-axis sensors (as illustrated in Fig. 1), they are not able to sense the acceleration vector of a single point unless the offsets in the position of the sensors is negligible. In fact, a triaxial sensor measures one-axis accelerations at three differ-

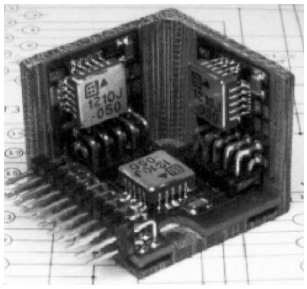

Figure 1: A triaxial accelerometer by Silicon Designs (©Silicon Designs).

ent locations and therefore gives an approximation of the spatial acceleration at the center of the unit. This drawback can be disregarded if the motion measured by the sensor is purely linear, but considerable errors are obtained with high-speed rotational motions as will be illustrated in Section 4. In the following sections, a robust design tackling this problem and increasing system robustness is presented.

3 Robust Design

3.1 IMU Kinematics Using Ideal Triaxial Accelerometers

A fundamental issue when designing IMU is the associated kinematics, i.e., the derivation of the motion parameters—namely the linear acceleration, angular acceleration and angular velocity of the IMU—from acceleration measurements.

To describe the general spatial motion of a rigid-body, let us consider an inertial frame ($\mathcal{F}$) and a body-attached frame ($\mathcal{B}$) as shown in Fig. 2. The accelerations of two arbitrary points of the rigid-body are related, i.e.,

$$\mathbf{a}_B = \mathbf{a}_A + \dot{\boldsymbol{\omega}} \times (\mathbf{r}_B - \mathbf{r}_A) + \boldsymbol{\omega} \times [\boldsymbol{\omega} \times (\mathbf{r}_B - \mathbf{r}_A)] \ , \quad (1)$$

where $\dot{\boldsymbol{\omega}}$ and $\boldsymbol{\omega}$ respectively denote the body angular acceleration and angular velocity; $\mathbf{r}_A$, $\mathbf{r}_B$, $\mathbf{a}_A$ and $\mathbf{a}_B$ are respectively the positions (with respect to the center of the body frame) and accelerations of points A and B. Then, n points of the body are referred to as P_i, with $i = 1, ..., n$. The vectors $\mathbf{r}_i$ and $\mathbf{a}_i$, with $i = 1, ..., n$, are respectively the position and acceleration vectors of point P_i. The centroid C of these points can be defined (Angeles 2002) as

$$\mathbf{r}_c = \frac{1}{n} \sum_{i=1}^{n} \mathbf{r}_i \ , \quad (2)$$

and the acceleration of the point attached to the body corresponding to C is

$$\mathbf{a}_c = \frac{1}{n} \sum_{i=1}^{n} \mathbf{a}_i \ . \quad (3)$$

Eq. (1) can be written considering all the points P_i associated with point C which yields

$$\mathbf{A} = \mathbf{W}\mathbf{R} \ , \quad (4)$$

where

$$\mathbf{A} = [\mathbf{a}_1 - \mathbf{a}_c \quad \mathbf{a}_2 - \mathbf{a}_c \quad ... \quad \mathbf{a}_n - \mathbf{a}_c] \ , \quad (5)$$

$$\mathbf{R} = [\mathbf{r}_1 - \mathbf{r}_c \quad \mathbf{r}_2 - \mathbf{r}_c \quad ... \quad \mathbf{r}_n - \mathbf{r}_c] \ , \quad (6)$$

and

$$\mathbf{W} \triangleq \dot{\boldsymbol{\Omega}} + \boldsymbol{\Omega}^2 \ , \quad (7)$$

where $\dot{\boldsymbol{\Omega}}$ and $\boldsymbol{\Omega}$ are the cross-product matrices corresponding to $\dot{\boldsymbol{\omega}}$ and $\boldsymbol{\omega}$, i.e.,

$$\dot{\boldsymbol{\Omega}} = \begin{bmatrix} 0 & -\dot{\omega}_z & \dot{\omega}_y \\ \dot{\omega}_z & 0 & -\dot{\omega}_x \\ -\dot{\omega}_y & \dot{\omega}_x & 0 \end{bmatrix} \ , \quad (8)$$

$$\boldsymbol{\Omega} = \begin{bmatrix} 0 & -\omega_z & \omega_y \\ \omega_z & 0 & -\omega_x \\ -\omega_y & \omega_x & 0 \end{bmatrix} \ . \quad (9)$$

Clearly, both matrices are skew-symmetric, and it is trivial to verify that $\boldsymbol{\Omega}^2$ is symmetric. $\mathbf{W}$ is the angular acceleration tensor of the rigid body.

Let us suppose that one ideal triaxial accelerometer (offsets are disregarded) is located at P_i, its output is

$$\mathbf{s}_i = \mathbf{Q}_i^{-1}\mathbf{a}_i - \mathbf{Q}_i^{-1}\mathbf{Q}^{-1}\mathbf{g} \ , \quad (10)$$

in which $\mathbf{g}$ is the gravitational acceleration expressed in the inertial frame, $\mathbf{Q}_i$ is the rotation matrix describing the orientation of the triaxial accelerometer relatively to $\mathcal{B}$, and $\mathbf{Q}$ is the rotation matrix describing the orientation of $\mathcal{B}$ relatively to $\mathcal{F}$. Solving the

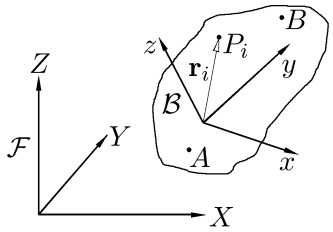

Figure 2: Inertial and body frames.

above equation for $\mathbf{a}_i$ and substituting it into eq. (3) and eq. (4) yields:

$$\mathbf{A} = \left[\mathbf{Q}_1\mathbf{s}_1 - \frac{1}{n}\sum_{i=1}^{n}\mathbf{Q}_i\mathbf{s}_i \quad \dots \quad \mathbf{Q}_n\mathbf{s}_n - \frac{1}{n}\sum_{i=1}^{n}\mathbf{Q}_i\mathbf{s}_i \right] \tag{11}$$

Then, the angular acceleration tensor of the rigid-body can be calculated using the pseudo-inverse of $\mathbf{R}$, i.e.,

$$\mathbf{W} = \mathbf{A}\mathbf{R}^T(\mathbf{R}\mathbf{R}^T)^{-1} \ . \tag{12}$$

Applying Cartesian decomposition to $\mathbf{W}$, one obtains

$$\dot{\mathbf{\Omega}} = \frac{1}{2}(\mathbf{W} - \mathbf{W}^T) \ , \tag{13}$$

$$\mathbf{\Omega}^2 = \frac{1}{2}(\mathbf{W} + \mathbf{W}^T) \ . \tag{14}$$

The angular acceleration of the rigid-body is readily obtained as

$$\dot{\boldsymbol{\omega}} = \mathrm{vect}(\dot{\mathbf{\Omega}}) \ . \tag{15}$$

Matrix $\mathbf{\Omega}^2$ can be written as

$$\begin{bmatrix} a & d & e \\ d & b & f \\ e & f & c \end{bmatrix} \ , \tag{16}$$

and using eq. (9), a set of six second-order equations is obtained, namely,

$$\begin{bmatrix} {\omega_y}^2 + {\omega_z}^2 \\ {\omega_x}^2 + {\omega_z}^2 \\ {\omega_x}^2 + {\omega_y}^2 \\ \omega_x\omega_y \\ \omega_x\omega_z \\ \omega_y\omega_z \end{bmatrix} = \begin{bmatrix} -a \\ -b \\ -c \\ d \\ e \\ f \end{bmatrix} \ . \tag{17}$$

If this set of equations is consistent, up to two solutions can be found. For example, if none of the three components of the angular velocity vector is zero, one has

$$\boldsymbol{\omega} = \pm \begin{bmatrix} \sqrt{(a-b-c)/2} \\ d\sqrt{2/(a-b-c)} \\ (f/d)\sqrt{(a-b-c)/2} \end{bmatrix} \ . \tag{18}$$

To determine the sign of the actual solution, the result of the previous time samples must be considered.

Knowing $\dot{\boldsymbol{\omega}}$ and $\boldsymbol{\omega}$, the linear acceleration of any point on the rigid-body can be computed by using eq. (1). Furthermore, the body frame attitude $\mathbf{Q}$ is updated by integrating the angular rate (Savage 1998).

Finally, the question of the minimal number of points required—and thus, the number of triaxial accelerometers—should be addressed. It is trivial to show that at least four non-coplanar sensors are required in the IMU: otherwise, the matrix $\mathbf{R}\mathbf{R}^T$ will be rank deficient and cannot be inverted.

3.2 The Case of Non-Ideal Triaxial Accelerometers

If n identical, non-ideal triaxial accelerometers are used in an IMU, a method to compensate for the errors caused by the offsets of the sensors should be used.

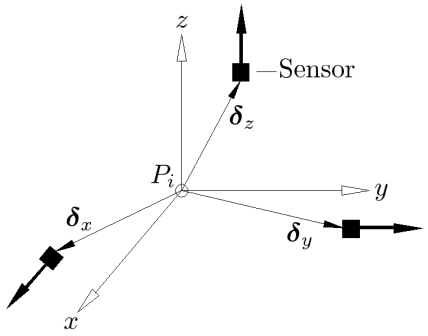

Figure 3: Illustration of a practical triaxial accelerometer.

As illustrated in Fig. 3, a triaxial accelerometer located at point P_i is composed of three single-axis sensors. For brevity's sake, the nominal center of the sensor is assumed to coincide with P_i. A local frame attached to P_i is formed by the three sensing axes. The position vectors of the three sensors with respect to the center of the local frame are

$$\begin{cases} \mathbf{r}_i^x = \mathbf{r}_i + \boldsymbol{\delta}_x \ , \\ \mathbf{r}_i^y = \mathbf{r}_i + \boldsymbol{\delta}_y \ , \\ \mathbf{r}_i^z = \mathbf{r}_i + \boldsymbol{\delta}_z \ , \end{cases} \tag{19}$$

where $\boldsymbol{\delta}_j$ is the position of the j-axis sensor with respect to P_i. Similarly to eq. (10), the outputs of these individual sensors are

$$\begin{cases} s_i^x = \mathbf{e}_x^T \mathbf{Q}_i^{-1}(\mathbf{a}_i + \mathbf{W}\boldsymbol{\delta}_x - \mathbf{Q}^{-1}\mathbf{g}) \ , \\ s_i^y = \mathbf{e}_y^T \mathbf{Q}_i^{-1}(\mathbf{a}_i + \mathbf{W}\boldsymbol{\delta}_y - \mathbf{Q}^{-1}\mathbf{g}) \ , \\ s_i^z = \mathbf{e}_z^T \mathbf{Q}_i^{-1}(\mathbf{a}_i + \mathbf{W}\boldsymbol{\delta}_z - \mathbf{Q}^{-1}\mathbf{g}) \ , \end{cases} \tag{20}$$

where $\mathbf{e}_x^T = [1\ 0\ 0]^T$, $\mathbf{e}_y^T = [0\ 1\ 0]^T$, $\mathbf{e}_z^T = [0\ 0\ 1]^T$, and $\mathbf{Q}_i$ describes the orientation of the local frame with respect to the body-frame. Then, the acceleration of point P_i approximated by the above three one-axis sensors is

$$\tilde{\mathbf{a}}_i = \mathbf{Q}_i \tilde{\mathbf{s}} + \mathbf{Q}^{-1}\mathbf{g} \ , \tag{21}$$

where $\tilde{\mathbf{s}} = [s_i^x \ s_i^y \ s_i^z]^T$, obtained from eq. (20).

It should be emphasized that $\tilde{\mathbf{a}}_i$ is not the true acceleration of P_i but only an approximation because of the elements $\mathbf{W}\boldsymbol{\delta}_j$ in its expression. The faster the rotation of the rigid-body is, the greater the magnitude of $\mathbf{W}$ becomes. The errors caused by $\mathbf{W}\boldsymbol{\delta}_j$ could be large enough that this approximation is unrealistic. Therefore, a procedure similar to the method presented in Section 3.1 cannot be used. To solve this issue, one can impose $\mathbf{Q}_i = \bar{\mathbf{Q}}$, with $i = 1, ..., n$, i.e., all the triaxial accelerometers share the same orientation. Then, an equation analogous to eq. (4) can be derived, i.e.,

$$\tilde{\mathbf{A}} = \mathbf{W}\mathbf{R} \tag{22}$$

where each column of $\tilde{\mathbf{A}}$ is

$$\bar{\mathbf{Q}}(\tilde{\mathbf{s}}_i - \frac{1}{n}\sum_{i=1}^{n} \tilde{\mathbf{s}}_i) \ . \tag{23}$$

It can be verified that all elements $\mathbf{W}\boldsymbol{\delta}_j$ in eq. (20) are canceled out in eq. (22), and thereby do not affect the computation. Hence, practical triaxial accelerometers of an IMU should have the same orientation, eliminating errors due to misplacements of the individual sensors.

3.3 IMU Error and Optimal Configuration

The causes of errors affecting an IMU can be separated in two categories: first, the measurement errors (scale factor error, bias and noise), and second, installation errors (position and orientation of the sensors). These errors should be identified and compensated with certain calibration to increase precision. Several methods have been proposed to this aim (Chen et al. 1994, Parsa et al. 2004). However, even after calibration, there are usually still residual errors and unmodeled measurement noise. In order to achieve a small sensitivity to these errors in the solution of eq. (12), the matrix $\mathbf{R}\mathbf{R}^T$ must have a small condition number. The condition number κ of a matrix $\mathbf{M}$ is defined as the ratio of its greatest to its smallest singular value (Golub and Van Loan 1996), i.e.,

$$\kappa(\mathbf{M}) = \frac{\sigma_l}{\sigma_s} \ . \tag{24}$$

A matrix is called isotropic and has minimum condition number ($\kappa = 1$) if its singular values are all identical and nonzero (Angeles 1986). Hence, for an IMU design, an optimal configuration is attained when $\mathbf{R}\mathbf{R}^T$ is isotropic. To find such a design leading to optimal conditioning, let $\mathbf{q}_i$ denotes $\mathbf{r}_i - \mathbf{r}_c$ in eq. (6), and let the matrix $\mathbf{M}$ be defined as

$$\mathbf{M} = \mathbf{R}\mathbf{R}^T = \sum_{i=1}^{n} \mathbf{q}_i \mathbf{q}_i^T \ . \tag{25}$$

A solution to render $\mathbf{M}$ isotropic consists in placing sensors at the vertices of Platonic solids (Baron and Angeles 1995). The five Platonic solids, namely, the tetrahedron $\mathcal{T}$, the octahedron $\mathcal{O}$, the cube $\mathcal{C}$, the icosahedron $\mathcal{I}$, and the dodecahedron $\mathcal{D}$ are associated with a certain number of triaxial sensors as summarized in Table 1.

Table 1: Optimal configurations.

Platonic solid	$\mathcal{T}$	$\mathcal{O}$	$\mathcal{C}$	$\mathcal{I}$	$\mathcal{D}$
Number of sensors	4	6	8	12	20

Although this solution provides a set of optimal design possibilities, it has obvious limitations. From the five designs in Table 1, the last two ($\mathcal{I}$ and $\mathcal{D}$) are impractical, for real implementation of these solutions in IMUs is cost prohibitive and leads to bulky designs. Furthermore, the geometry of Platonic solids sheds no light on IMUs with five or seven sensors,

which are very likely to be considered. Indeed, a five-sensor design is very interesting, as it is the first redundant case of IMU design. An optimization technique can be used to obtain the design minimizing the condition number of $\mathbf{M}$. To this purpose, let us consider a design augmented from the $\mathcal{T}$ setup and within the boundaries of a cube having edge lengthes of l. As illustrated in Fig. 4, the first four points form a regular tetrahedron, and the fifth point is to be determined for an optimal configuration. This optimization problem can be formulated as

$$\min_{\mathbf{r}_5 \in \mathbb{R}^3} \kappa(\mathbf{M}) \tag{26}$$

subject to $[0\ 0\ 0]^T \leq \mathbf{r}_5 \leq [l\ l\ l]^T$, where $\mathbf{r}_5$ is the position of the fifth point.

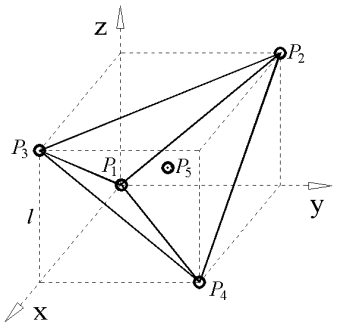

Figure 4: Optimal design with five sensors.

The above problem is solved numerically using a technical computing software. The location obtained of the fifth sensor is $\mathbf{r}_5 = [\frac{l}{2}\ \frac{l}{2}\ \frac{l}{2}]^T$, i.e., the center of the tetrahedron. The resulting condition number of $\mathbf{M}$ is 1, meaning an isotropic design has been found.

3.4 System Reliability

As mentioned previously, the minimal number of triaxial accelerometers required to handle the computation is four. To enhance reliability and improve system performance, redundancy is desired in the IMU implementation. During the operation of the IMU, if a sensor fails, its output should be disregarded. In particular, the computation scheme formerly derived must be updated, taking into account this possible failure, as illustrated in Fig. 5.

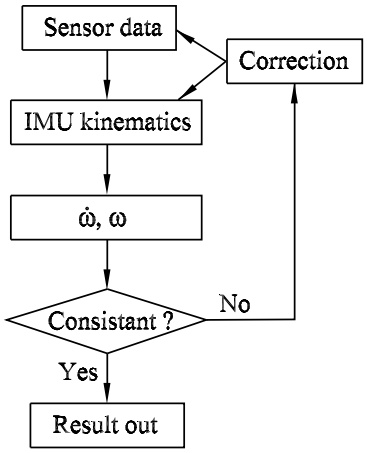

Figure 5: IMU operation flow chart.

Regarding the method to detect sensor failure, eq. (17) can be analyzed. If the IMU is assumed to be precisely manufactured and calibrated, then the two sets of values of the angular velocity solved using the first three and the last three equations should be identical or of little discrepancy. However, if the two solutions are significantly different, it indicates that a sensor is damaged. Specifically, this consistency can be defined as

$$\|\boldsymbol{\omega}_1 - \boldsymbol{\omega}_2\|_\infty < \epsilon\ , \tag{27}$$

where $\boldsymbol{\omega}_1 = [\omega_{x,1}\ \omega_{y,1}\ \omega_{z,1}]^T$ is solved from the first three equations of eq. (17) and $\boldsymbol{\omega}_2 = [\omega_{x,2}\ \omega_{y,2}\ \omega_{z,2}]^T$ from the last three. The scalar ϵ is a tolerance index. Therefore, by monitoring the consistency criterion during the operation of the IMU, a navigation computer is able to assess the functionality of the sensors in the IMU.

To update the computation algorithm, two types of failures have to be differentiated. If a failure happens to a triaxial sensor, the computation program can be modified to discard that sensor. On the other hand, if only one element or two of a triaxial sensor fail, the others can still be used and a new computation algorithm must be established as follows.

Because each triaxial accelerometer has the same orientation, supposed to be aligned with the body-frame, all the sensing elements in the IMU can be classified into three groups, namely, group x, group

y and group z. In group x, the axis of each sensing element is parallel to the x axis of the body-frame. Similarly, the axes of the sensor groups y and z are parallel to the y and z axes of the body-frame. It is worth noting that the number of sensing elements in each group are not necessarily equal because of sensor failures. Let us consider the relationship between the point acceleration of a sensor in group x and the acceleration of the origin of the body-frame, one has

$$\mathbf{a}_i^x = \mathbf{a}_o + \mathbf{W}\mathbf{r}_i^x \tag{28}$$

where $\mathbf{a}_o = [a_x \ a_y \ a_z]^T$ is the acceleration of the origin of the body-frame, $\mathbf{r}_i^x$ and $\mathbf{a}_i^x$ are respectively the position and the acceleration of the point corresponding to the position of sensor i, and $\mathbf{W} = [\mathbf{w}_1 \ \mathbf{w}_2 \ \mathbf{w}_3]^T$ is the angular acceleration tensor. Then, the output of the sensor can be calculated, i.e.,

$$s_i^x = a_x + \mathbf{w}_1^T\mathbf{r}_i^x - \mathbf{e}_x\mathbf{Q}^{-1}\mathbf{g} \ ,$$

which can be rewritten into

$$s_i^x + \mathbf{e}_x\mathbf{Q}^{-1}\mathbf{g} = \begin{bmatrix} 1 & (\mathbf{r}_i^x)^T \end{bmatrix} \begin{bmatrix} a_x \\ \mathbf{w}_1 \end{bmatrix} \ . \tag{29}$$

Similarly, two more equations are obtained for group y and z, namely,

$$s_j^y + \mathbf{e}_y\mathbf{Q}^{-1}\mathbf{g} = \begin{bmatrix} 1 & (\mathbf{r}_j^y)^T \end{bmatrix} \begin{bmatrix} a_y \\ \mathbf{w}_2 \end{bmatrix} \ , \tag{30}$$

and

$$s_k^z + \mathbf{e}_z\mathbf{Q}^{-1}\mathbf{g} = \begin{bmatrix} 1 & (\mathbf{r}_k^z)^T \end{bmatrix} \begin{bmatrix} a_z \\ \mathbf{w}_3 \end{bmatrix} \ . \tag{31}$$

Eqs. (29)-(29) can be written for all sensors of each group and one obtains

$$\mathbf{D}\mathbf{f} = \mathbf{s}_g \ , \tag{32}$$

where $\mathbf{D}$ contains the information about the sensor positions, $\mathbf{s}_g$ is a vector containing the sensor outputs and the effect of gravity, and $\mathbf{f}$ is the vector of unknown parameters. In detail, one has

$$\mathbf{D} = \begin{bmatrix} \mathbf{D}_x & & \mathbf{0} \\ & \mathbf{D}_y & \\ \mathbf{0} & & \mathbf{D}_z \end{bmatrix} \ , \tag{33}$$

with

$$\mathbf{D}_x = \begin{bmatrix} 1 & (\mathbf{r}_1^x)^T \\ \vdots & \vdots \\ 1 & (\mathbf{r}_l^x)^T \end{bmatrix} \ , \tag{34}$$

where l denotes the number of sensors in group x. Similarly to eq. (34), $\mathbf{D}_y$ and $\mathbf{D}_y$ can be defined as

$$\mathbf{D}_y = \begin{bmatrix} 1 & (\mathbf{r}_1^x)^T \\ \vdots & \vdots \\ 1 & (\mathbf{r}_m^x)^T \end{bmatrix}, \ \mathbf{D}_z = \begin{bmatrix} 1 & (\mathbf{r}_1^x)^T \\ \vdots & \vdots \\ 1 & (\mathbf{r}_n^x)^T \end{bmatrix} . \tag{35}$$

Vector $\mathbf{s}_g$ is defined as

$$\mathbf{s}_g = \mathbf{s} + \mathbf{u} \ , \tag{36}$$

where

$$\mathbf{s} = [s_1^x \ ... \ s_l^x \ \ s_1^y \ ... \ s_m^y \ \ s_1^z \ ... \ s_n^z]^T \ , \tag{37}$$

and

$$\mathbf{u} = [\mathbf{e}_x\mathbf{Q}^{-1}\mathbf{g} \ ... \ \mathbf{e}_y\mathbf{Q}^{-1}\mathbf{g} \ ... \ \mathbf{e}_z\mathbf{Q}^{-1}\mathbf{g} \ ...]^T \ . \tag{38}$$

Finally, $\mathbf{f}$ is the vector of unknowns, namely,

$$\mathbf{f} = [a_x \ \mathbf{w}_1^T \ a_y \ \mathbf{w}_2^T \ a_z \ \mathbf{w}_3^T]^T \ ,$$

and can be obtained using the pseudo-inverse of $\mathbf{D}$, i.e.,

$$\mathbf{f} = (\mathbf{D}^T\mathbf{D})^{-1}\mathbf{D}^T\mathbf{s}_g \ . \tag{39}$$

Hence, the acceleration of the origin of the body-frame $[a_x \ a_y \ a_z]^T$ is readily at hand. Referring to Section 3.1, $\dot{\boldsymbol{\omega}}$ and $\boldsymbol{\omega}$ can be obtained from $\mathbf{W}$.

The above algorithm not only solves the situation when failure(s) of sensing element(s) occur(s), but also offers more insights for the design of IMUs. It implies that a design based on triaxial accelerometers can be extended to a more general scheme, in which all sensing elements are divided into three groups with axes orthogonal to each other. Hence, aside from the triaxial sensor, one- or two-axis sensors can also be integrated into the IMU to provide sensing elements, lending more design flexibility.

4 Simulation Results

SimMechanics^{TM}, a toolbox of Matlab^{TM}, is a block diagram modeling environment for the design and simulation of rigid body machines. The theoretical analysis in Section 2 and 3 can be validated with the example of a 6 degrees of freedom (DOF) serial robot. The block diagram of the virtual robot modeled using SimMechanics^{TM} is illustrated in Fig. 6. The *Denavit-Hartenberg* (DH) parameters of this robot are specified in Table 2.

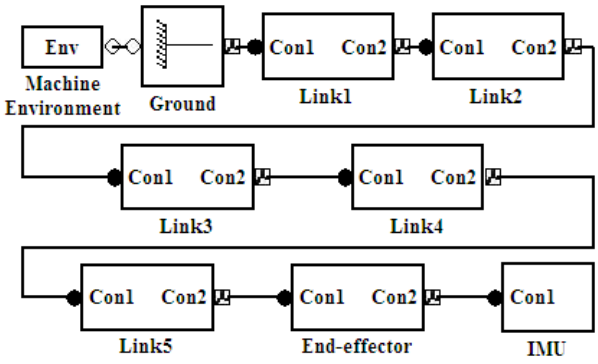

Figure 6: Modeling of a six-dof serial robot equipped with an IMU.

Table 2: DH parameters [m, rad].

	a	d	θ	α
1	0.95	0	θ_1	$-\pi/2$
2	0.7	0	θ_2	0
3	0.3	0	θ_3	$-\pi/2$
4	0	0.65	θ_4	$\pi/2$
5	0	-0.4	θ_5	$-\pi/2$
6	0	0.8	θ_6	0

To verify the proposed IMU computation algorithms, hypotheses are made, namely the system has no installation errors or measurement noise. In this simulation, an IMU containing four ideal triaxial accelerometers in the $\mathcal{T}$ layout is tested. The orientations of the sensors are identical in the body-frame. The robot is commanded to follow a trajectory and its end-effector undergoes a spatial motion. During the simulation, the true values of the motion parameters, i.e., angular acceleration, angular velocity and linear acceleration of the body-frame's origin, are recorded by software. In the meantime, the virtual measurements of linear accelerations at the four sensors are sampled and sent to the IMU computation algorithm. Finally, the computed motion parameters are compared to the recorded true values. For instance, Fig. 7 shows that the computed angular accelerations (dots) coincide exactly with the true values (solid line).

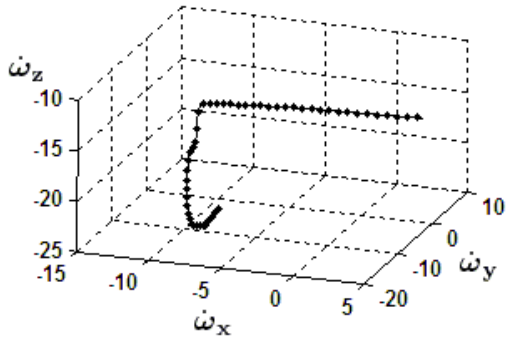

Figure 7: Computed and actual angular accelerations during an arbitrary trajectory.

Afterwards, to investigate the non-ideal triaxial accelerometer case, each sensor is assumed to have an arbitrary orientation and have offsetted sensing elements. The offsets are chosen identical for all the sensing elements and equal to one-hundredth of the tetrahedron's edge length. In order to compare the computed angular velocities and accelerations ($\boldsymbol{\varpi}_c^T = [\boldsymbol{\omega}_c^T \ \dot{\boldsymbol{\omega}}_c^T]$) of the IMU with the corresponding real values ($\boldsymbol{\varpi}_t^T = [\boldsymbol{\omega}_t^T \ \dot{\boldsymbol{\omega}}_t^T]$), let us define the error between them as

$$e = \|\boldsymbol{\varpi}_c - \boldsymbol{\varpi}_t\|_2 \ , \tag{40}$$

and the relative error as

$$e_r = \frac{\|\boldsymbol{\varpi}_c - \boldsymbol{\varpi}_t\|_2}{\|\boldsymbol{\varpi}_t\|_2} \ . \tag{41}$$

The trajectory used in Fig. 7 is rerun with these configuration changes, and significant errors are obtained as shown in Fig. 8. The necessity of the robust scheme discussed in Section 3.2 is therefore reinforced. Indeed, these errors can be completely eliminated by using the proposed robust design.

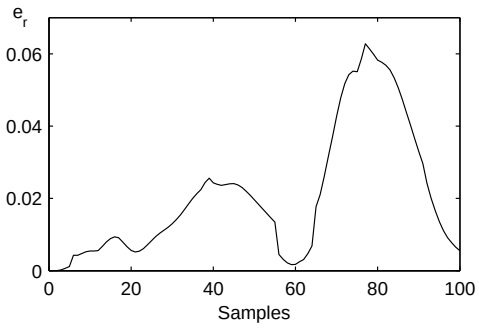

Figure 8: Relative error e_r.

The effectiveness of redundancy can also be investigated. For instance, let us compare designs with four, six and eight triaxial accelerometers. Referring to Fig. 9, the four-sensor IMU consists in a regular tetrahedron ($P_1P_2P_3P_4$); the six-sensor design is composed of six centers of the cube faces, forming an Octahedron; and finally, all the vertices of the cube are used in the eight-sensor design. Subsequently, orientation errors in the alignment of accelerometers are generated. The values of the roll, pitch, and yaw angles of the sensing axis are supposed to be randomly distributed between $-3°$ and $3°$ of the theoretical value. One hundred samples are collected from simulations for each IMU design. As an example, the errors of angular accelerations during an arbitrary trajectory is plotted in Fig. 10, and the average/maximal values of e_r are summarized in Table 3. It is clearly seen that the accuracy of the computed results as well as the maximal errors are improved when a larger number of sensors is used. Moreover, many other tests have been done with different trajectories, and repeatedly confirmed the effectiveness of the proposed redundancy design.

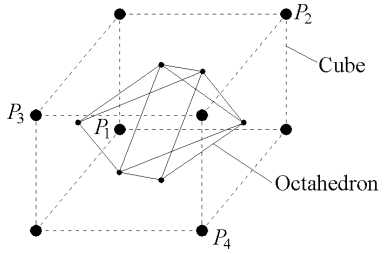

Figure 9: Three designs derived from the vertices of a cube.

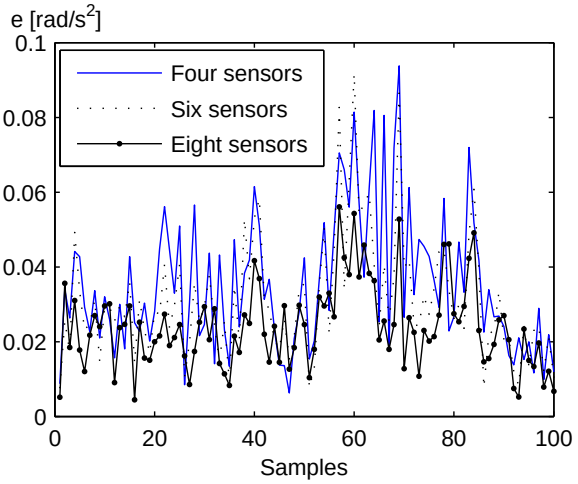

Figure 10: The error e of angular accelerations during the trajectory.

Table 3: Redundancy study results.

Number of sensors	Four	Six	Eight
Average values of e_r	6.53%	6.07%	4.86%
Maximal values of e_r	17.3%	12.7%	7.95%

5 Conclusion

This paper has presented the robust design scheme to realize IMUs based on accelerometers. The system obtained has several advantages: (1) the proposed IMUs can directly determine the angular velocity of the sensor without integrating the angular acceleration, thereby increasing the accuracy; (2) the errors due to sensor offsets in triaxial accelerometers can be eliminated by choosing a unique orientation for all the sensors in the design; (3) the robustness of the computation to installation errors and measurement noise is enhanced by redundancy and optimal configuration of sensors; (4) the system reliability guarantees the IMU's functionality in case of sensor failure(s). The theoretical analysis conducted in this paper has been verified with computer simulations. These simulations showed the validity of the presented IMU computation algorithms and the ef-

fectiveness of system redundancy in coping with IMU errors.

References

Angeles, J.: 1986, Automatic computation of the screw parameters of rigid-body motions. part 1: Finitely-separated positions., *Journal of Dynamic Systems, Measurement and Control, Transactions ASME* **108**(1), 32 – 38.

Angeles, J.: 2002, *Fundamentals of Robotic Mechanical Systems: Theory, Methods, and Algorithms*, second edn, Springer.

Baron, L. and Angeles, J.: 1995, Isotropic decoupling of the direct kinematics of parallel manipulators under sensor redundancy, *Proceedings of IEEE International Conference on Robotics and Automation*, Vol. 2, Nagoya, Jpn, pp. 1541 – 1546.

Chen, J.-H., Lee, S.-C. and DeBra, D. B.: 1994, Gyroscope free strapdown inertial measurement unit by six linear accelerometers, *Journal of Guidance, Control, and Dynamics* **17**(2), 286 – 290.

DiNapoli, L.: 1965, *The measurement of angular velocities without the use of gyros*, Master's thesis, University of Pennsylvania, Philadelphia.

Golub, G. H. and Van Loan, C. F.: 1996, *Matrix Computations*, third edn, The Johns Hopkins University Press, Baltimore.

Li, G., Li, Z., Wang, C., Hao, Y., Li, T., Zhang, D. and Wu, G.: 2001, Design and fabrication of a highly symmetrical capacitive triaxial accelerometer, *Journal of Micromechanics and Microengineering* **11**(1), 48 – 54.

Liu, Y.: 1976, Letter to the editor on: measurement of angular acceleration of a rigid body using linear accelerometers by padgaonkar et al., *Journal of Applied Mechanics* **43**, 377 – 378.

Matsumoto, Y., Nishimura, M., Matsuura, M. and Ishida, M.: 1999, Three-axis soi capacitive accelerometer with pll c-v converter, *Sensors and Actuators, A: Physical* **75**(1), 77 – 85.

Mostov, K. S., Soloviev, A. A. and Koo, T.-K. J.: 1997, Accelerometer based gyro-free multi-sensor generic inertial device for automotive applications, *IEEE Conference on Intelligent Transportation Systems, Proceedings, ITSC*, Boston, MA, USA, pp. 1047 – 1052.

Padgaonkar, A. J., Krieger, K. W. and King, A. I.: 1975, Measurement of angular acceleration of a rigid body using linear accelerometers., *Journal of Applied Mechanics, Transactions ASME* **42 Ser E**(3), 552 – 556.

Parsa, K., Angeles, J. and Misra, A. K.: 2004, Rigid-body pose and twist estimation using an accelerometer array, *Archive of Applied Mechanics* **74**(3 - 4), 223 – 236.

Plaza, J., Chen, H., Esteve, J. and Lora-Tamayo, E.: 1998, New bulk accelerometer for triaxial detection, *Sensors and Actuators, A: Physical* **66**(1-3), 105 – 108.

Savage, P.: 1998, Strapdown inertial navigation integration algorithm design. 1. attitude algorithms, *Journal of Guidance, Control, and Dynamics* **21**(1), 19 – 28.

Schuler, A., Grammatikos, A. and Fegley, K.: 1965, Measuring rotational motion with linear accelerometers, *IEEE East Coast Conference on Aerospace and Navigational Electronics*.

Yazdi, N., Ayazi, F. and Najafi, K.: 1998, Micromachined inertial sensors, *Proceedings of the IEEE* **86**(8), 1640 – 1658.

View publication stats